Shahid Beheshti University

Sustainable Earth Review

Journal homepage: http://sustainearth.sbu.ac.ir

Source Parameters and Rupture characteristics of the 2017 earthquake in Kermanshah, Iran

Farzaneh Mohammadi[a], Hesaneh Mohammadi[b*], Mohammad Reza Gheitanchi[a]

[a] Institute of Geophysics, Department of Seismology, University of Tehran, Tehran, Iran
[b] Department of Geophysics, Tehran North Branch, Islamic Azad University, Tehran, Iran

ABSTRACT

The Empirical Green Function and the Stochastic Finite-Fault Simulation were applied to estimate source parameters and rupture process of the November 12, 2017, earthquake with a moment magnitude of 7.3 in Ezgeleh, Kermanshah, Iran. The Ezgeleh earthquake was one of the most destructive and complex events that have occurred in this region; it seems several parallel faults have been activated. We determined the focal mechanism of the main event using first motion polarities. The result shows reverse faulting with a small strike-slip component. Also, the size of the asperity in this earthquake was estimated to be about 55km in the strike direction and 25km in the dip direction. To simulate this event, corner frequency, seismic moment, stress drop, duration, and the causative fault plane model were estimated. The simulated strong ground motions in comparison with the observed ones show good agreement; the result shows that the applied rupture model for this earthquake and the synthesizing methods are effective at simulating near-source ground motions in a broad-frequency range of engineering interest. Moreover, these approaches are successful and efficient in predicting the strong motions in the Zagros fold and thrust belt. This earthquake shows us that in areas with tectonics and seismic behavior similar to those of the Zagros fold and thrust belt, the possibility of such earthquakes is not unexpected. Therefore, it is necessary to simulate probable large earthquakes for the high safety design of these areas.

ARTICLE INFO

Keywords:
Focal Mechanism
Empirical Green Function
Source Parameters
Stochastic Finite Fault Simulation

Article history:
Received: 04 Jan 2022
Accepted: 08 Mar 2022

*corresponding author
E-mail address:
h.mohammadi@iau-tnb.ac.ir
(H. Mohammadi)

1. Introduction

On November 12, 2017, an earthquake with a Moment magnitude (Mw) of 7.3 occurred in the vicinity of Sarpol-e-Zahab town, Kermanshah, Iran (Ezgeleh earthquake). This earthquake has been the largest event in this region in the Zagros Fold-Thrust Belt between the Arabian and Eurasian plates, in the last hundred years; the previous largest event in the area had occurred in 1909 in Silakhor, near the Borujerd city in the Zagros region, with a magnitude of 7.4 (Ambraseys and Melville, 2005). The Zagros region, including the Zagros fold belt and high Zagros with some of the important structural faults, is one of the most seismically active regions in Iran (Talebian and Jackson, 2004).

The existence of several faults, such as the Main Zagros Fault (MZF), Zagros Mountain Front Fault (MFF), High Zagros Fault (HZF), and dozens of other important and fundamental faults make this region seismically active. In the Zagros structural domain, the MFF is a basement thrust fault (dipping NE) and the HZF is a reverse fault with a small dextral component (dipping NE). In general view, most of the Zagros active thrust faults play a role as blind faults (Berberian, 1995). Zagros, which is now under the influence of a convergent pattern due to tectonic pressures with north- northeast and south-southwest trends, is located in the central portion of the Arabia-Eurasia young collision zone (Berberian, 1995). This increasing tension causes the accumulation of energy in the region and, consequently, the occurrence of earthquakes.

Mostly, these earthquakes are rather shallow with a magnitude of less than 6 that have a short return period. Usually, the depth of earthquakes in Zagros is less than 30 kilometers (Niazi et al., 1978; Jackson and Fitch, 1981; Talebian and Jackson, 2004; Nissen et al., 2011; Karasözen et al., 2019). The Seismicity map of the study area is illustrated in figure 1.

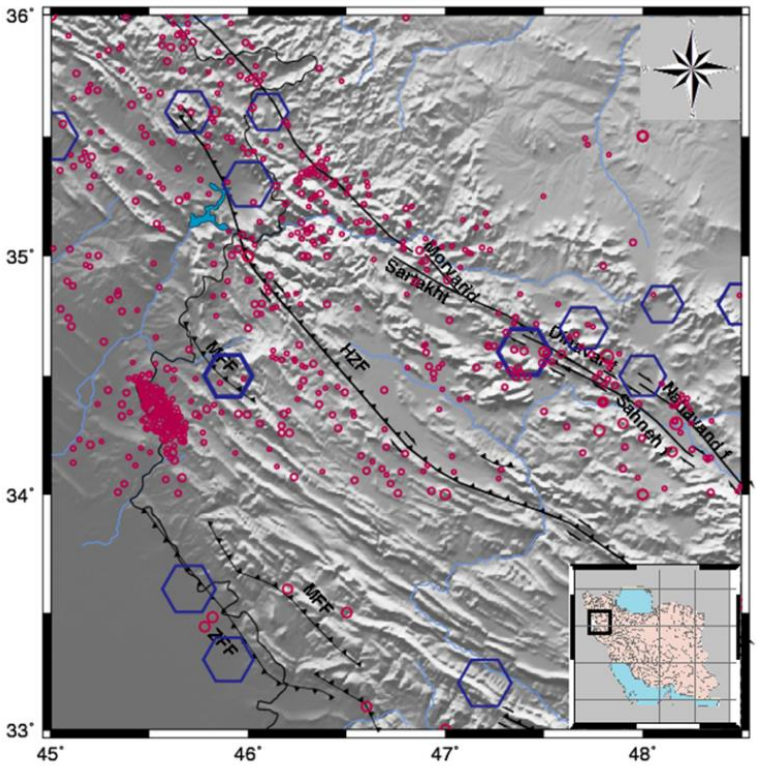

Fig.1. The seismicity map of the study area. The historical large earthquakes in this region are shown by hexagons. The instrumental events are demonstrated by circles with different sizes relative to their magnitudes.

The Ezgeleh earthquake was located in the vicinity of MFF. In this study, near-source data were used to estimate the source parameters of this earthquake. Ground motions records are distance dependent (Shakal and Bernreuter, 1980; Theodulidis and Papazachos, 1992; Imtiaz et al., 2015). The spatial and temporal distribution of slip can be obtained more precisely using near-source ground motion records which are influenced by directivity, near-source pulse motion, and static offsets (Raghukanth, 2008; Wan et al., 2022). This event caused structural damage and loss of lives. Some of the structures in this region are highly vulnerable to earthquake shaking since those structures were built on alluvial soils. Reportedly, in three months, more than 1500 aftershocks were recorded by the Iranian seismological center (IRSC) for this earthquake. In this paper, the Empirical Green Function method and Stochastic Finite-Fault modeling were applied to simulate strong ground motion, to evaluate the effectiveness of these methods in synthesizing earthquakes in this region.

2. Material and Methods

The Ezgeleh earthquake was recorded by 109 near-source stations of Iran Strong Motion Network (ISMN) across the country. The maximum recorded acceleration of this event was recorded at Sarpol-e Zahab station with an acceleration of about 684cm/s^2 for the north-south component. Using Peak Ground Accelerations (PGA) recorded by the near-field stations, the distribution of PGAs, corresponding to the event was estimated. The spatial distribution of PGAs corresponding to the Ezgeleh earthquake is demonstrated in figure 2.

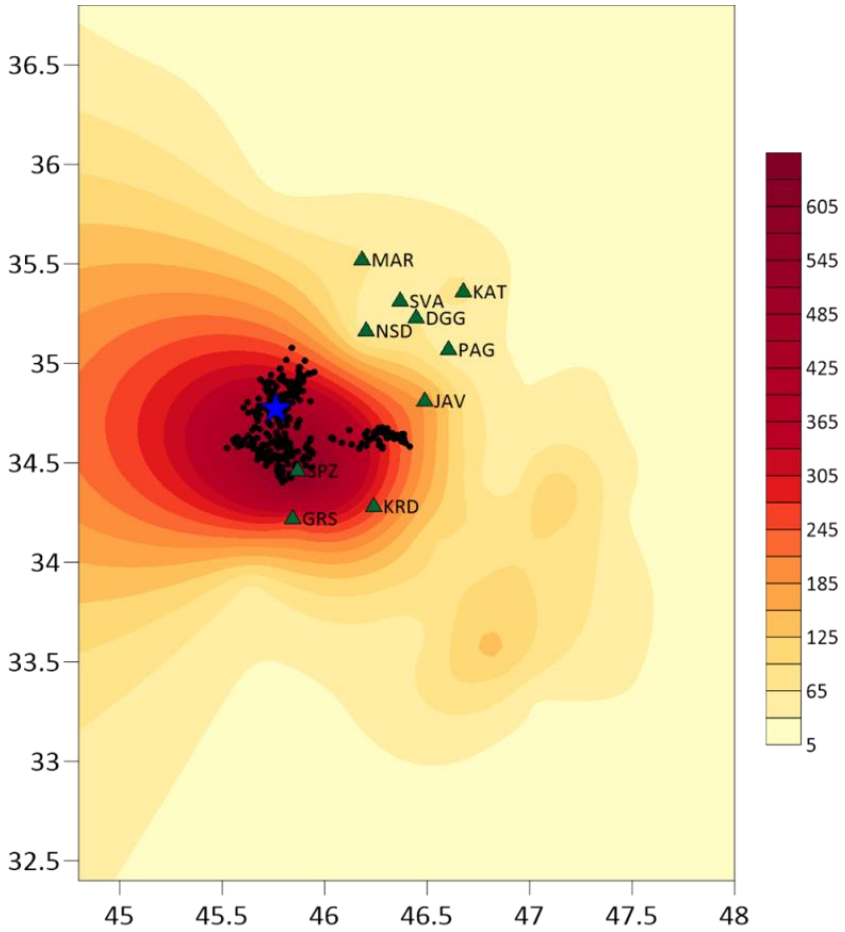

Fig.2. Spatial distribution of PGAs corresponding to the Ezgeleh earthquake. The main event is shown by a star; also the aftershocks and the stations are demonstrated by circles and triangles, respectively

In this study, to simulate the target event, the records with a source to site distances within 100km were selected. The quality of each record was evaluated based on the signal-to-noise ratio technique (SNR≥3). Before using accelerograms, data processing, including baseline correction and filtering, is essential (Alexander et al., 2001; Boore and Bommer, 2005). Data were analyzed by applying a linear correction to resolve the divergence from the baseline; moreover, the raw signals were band-pass filtered between 0.2 and 25Hz by the 4^{th} order of the Butterworth filter, owing to the fact that this frequency band demonstrates the main characteristics of the ground motion. The filtering helped baseline correction too. Stress drop $(\Delta\sigma)$ which is the difference between the stress across the fault before and after an earthquake rupture was calculated for this event using the corner frequency and seismic moment; the stress drop is defined as:

$$\Delta\sigma = \frac{7.0\times10^{-16}}{16\times(0.37V_r)^3} M_0 f_0^3 \qquad (1)$$

In equation (1), M_0 is the scalar seismic moment and f_0 is the corner frequency of this earthquake; in this study, M_0 and f_0 were determined using the Fourier Spectrum on a logarithmic scale to be $1.34\times10^{20}\,\mathrm{N.m}$ and 0.5Hz, respectively. V_r is rupture velocity and can be taken as 0.8 times of shear velocity in the crust (Somerville et al., 1999).

2.1. Empirical Green Function method

Theoretically, Green functions are the impulse response of the medium; and Empirical Green Functions (EGFs), are recordings used to provide this impulse response. In 1978, Hartzell and Wu proposed applying small earthquakes as EGFs to estimate strong ground motion. Using small events to provide EGFs is an effective approach to simulate large earthquakes as small events occur more frequently than large events (Hartzell, 1978; DeLorenzo et al., 2007; Honoré et al., 2011; Yoshida et al., 2022); Hartzell and Wu suggested using EGFs as the Green function in the representation relation along with synthetic rupture processes for calculating the resulting ground motion. In this method, the fault of a large earthquake is represented as a

summation of sub faults, or elemental point sources, for which EGFs are available. In 1984, Irikura suggested using a large event as an EGF and modified it to illustrate the strong ground motion from an even larger earthquake with at least the magnitude difference of approximately 1 unit. In this method, the EGF is not considered as a point source, and the larger event is a summation of relatively large sub-events (Hartzell, 1978; Wu, 1978; Hutchings, 1987; Hutchings and Viegas, 2012). In this technique, to simulate the target (main) event, an element (small) event, which is usually a foreshock or aftershock of an earthquake, is used. The empirical Green function method shows that recordings of small events contain the propagation characteristics which are necessary for modeling large nearby earthquakes. For utilizing this approach, several criteria were distinguished to find applicable small events; the focal mechanism of the element and the target event should be similar (Irikura, 1991). The hypocenter of each event is presumed to be identical in the EGF method; as a result, waves generated by those events go along the same path (Courboulex et al., 1996). Also, the difference in magnitudes must be larger or equal to 1; both events must be recorded at a minimum of three common stations, which must be well distributed in azimuth around the epicenter.

2.2. Stochastic Finite-Fault (SFF) Method

The stochastic simulation technique developed by Motazedian and Atkinson (2005) was employed in this study. The technique is known to be effective for high-frequency (>0.1Hz) ground motions required for structural engineering purposes (Campbell and Bozorgnia, 2006). This approach is based on introducing dynamic corner frequencies. This method requires detailed knowledge of the path and site effects; Input parameters are based on the characteristics of both the source and the path (seismic velocities and attenuation in the crust). The path attenuation is quantified by the quality factor, and geometric spreading function. In this study, the quality factor evaluated in this region by Rezapour et al. (2018) and a constant stress drop calculated to be 700 bars were used. In this simulating approach, seismic moment, stress drop, rupture dimension, velocity and propagation properties, and distribution of slip are included in the modeling. In the stochastic finite-fault method, the main fault is illustrated as the sum of the number of segments that are considered as point sources (Hartzell, 1978).

3. Results and discussion

In this study, We determined the focal mechanism of the main event using first motion polarities, the result shows reverse faulting with a small strike-slip component; according to the criteria explained in the previous section, a small event that has a focal mechanism similar to that of the main event should be selected as the empirical Green function; in this case, because of the high scattering of aftershocks (located by Iranian Seismological Center (IRSC)) that could be the result of multiple small ruptures, the main causative fault plane was not easily recognizable (Figure 3.A); therefore, we used relocated aftershocks by Mohammadi and Moradi (2019) using Double Difference Earthquake Location Method, which minimizes errors due to unmodeled velocity structure. The relocation results revealed a more focused picture of the distribution of aftershocks (Figure 3 B). Finally, to satisfy the mentioned criteria, we have selected 4 common stations at which the main event and the aftershock, applied as the empirical Green function, were recorded. The focal mechanism of the main earthquake (target event) and its aftershock (element event), selected as the Green function, is shown in figure 3.B; also, the location of four stations with different azimuth coverage at which both target and element events were recorded can be seen on this map. Furthermore, the distribution of relocated about 400 aftershocks is demonstrated in figure 3.

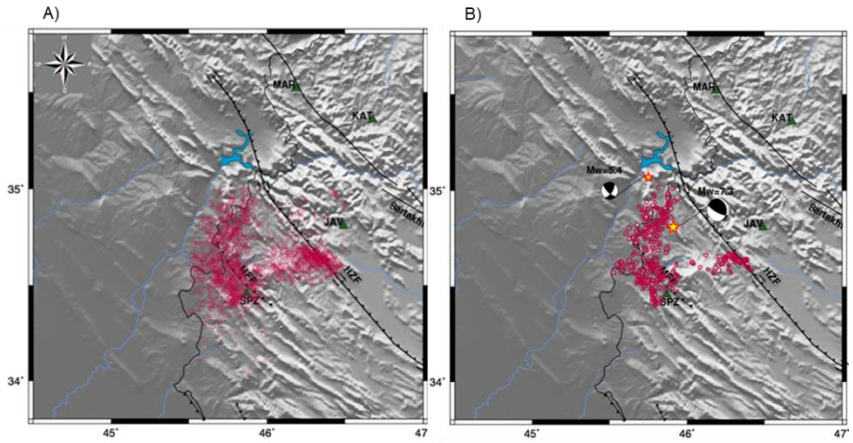

Fig.3. The comparison between IRSC locations and relocated data. A) IRSC Locations of aftershocks. B) The distribution of relocated aftershocks and the focal mechanisms of the target and the small event, which was selected as the Green function, and the four common stations at which both events were recorded. The aftershocks and the stations are demonstrated by circles and triangles, respectively (Mohammadi and Moradi, 2019)

Strong ground motion synthesis with EGFs has been the subject of research and application for many years. In this study, our primary interest is in using the EGF method for engineering purposes; to serve this purpose, the frequency band of interest is about 0.2 to 25Hz. Considering the focal mechanism of the mainshock and the distribution of relocated aftershocks, the causative fault of the Ezgeleh earthquake has a slope towards NE direction; the nodal plane with Strike, dip, and rake of 348, 27, and 137 degrees, respectively, was chosen as the main fault plane. Figure 4 illustrates a model of the causative fault plane of the target event. The rupture was generated from the element (16 5), which is illustrated in figure 4, on the fault plane at the depth of 8 km and unilaterally propagated from the hypocenter from northwest to southeast direction; it is in agreement with the trend of faults in this area.

In this paper, the fault rupture dimensions were calculated using the equations estimated by Wells and Coppersmith (1994). The size of the main fault and sub-fault (element) was estimated according to the rupture area of the main event and small event, respectively. In this technique, the main causative fault is divided into sub faults of equal size. The number of sub faults was calculated using the magnitude and the focal mechanism of the small event selected as the Green function for this earthquake. The size of the asperity in this earthquake is about 55km in the strike direction and 25km in the dip direction. The sub-fault length in the strike direction is about 3.5km and its width is 4km. The duration of events is influenced by the rupture dimensions and its process. Considering the fault length along the strike direction and the rupture velocity assumed to be 2.56 cms, the duration of this earthquake is about 22 seconds.

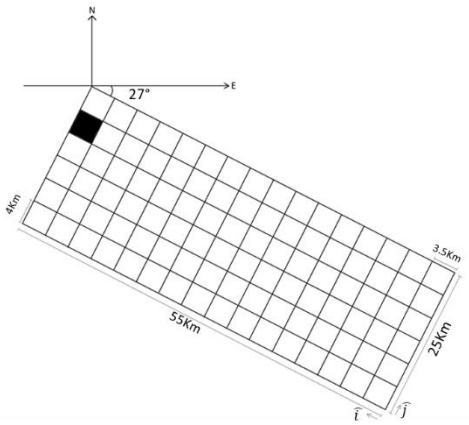

Fig. 4. The causative fault plane model of the earthquake

After simulating the earthquake by applying EGF and SFF methods, the observed records and the simulated graphs were compared. The comparison of the observed (OBS) and

synthetic (SYN) diagrams of acceleration is demonstrated in figure 5. In figure 6, we present the results of the simulation and their comparisons with the observed Fourier and the 5% damped pseudo-acceleration Response spectra of the earthquake in the North-South (N-S) direction for all selected stations. Also, the peak values of the observed and simulated records of the Ezgeleh earthquake are shown in table 1.

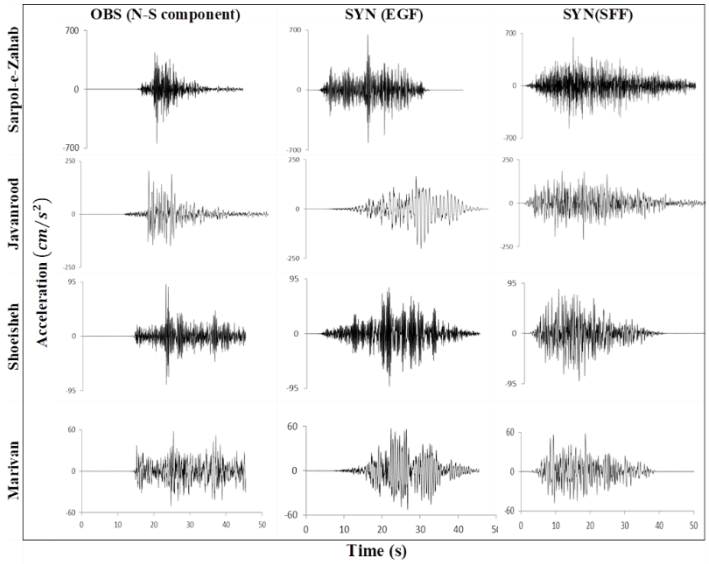

Fig. 5. Observed and synthetic acceleration diagrams of the main event in the North-South component of the near field stations

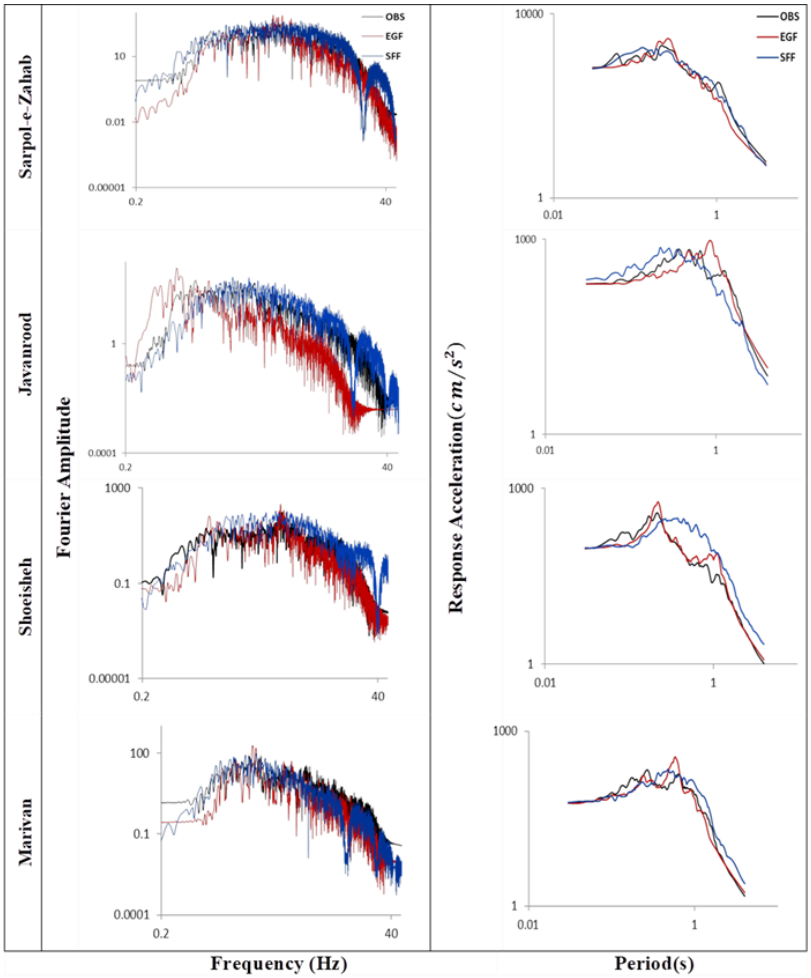

Fig. 6. Observed and synthetic Fourier and acceleration response spectra of the main event in the North-South component of the stations

Table 1. The peak values of the observed and simulated diagrams of the earthquake in four stations

Station	Parameter	Observed	Synthetic (SFF)	Synthetic (EGF)
Sarpol-e-Zahab (SPZ)	PGA(cm/s^2)	648.41	650.53	646.47
	PGV(cm/s)	21.35	19.89	27.606
	PGD(cm)	2.08	1.82	1.42
	Duration(s)	10.45	30.34	22.25
Javanrood (JAV)	PGA(cm/s^2)	204.05	211.71	202.56
	PGV(cm/s)	17.21	15.79	23.67
	PGD(cm)	2.60	3.27	3.66
	Duration(s)	16.64	27.51	17.33
Shoeisheh (KAT)	PGA(cm/s^2)	91.07	89.94	91.64
	PGV(cm/s)	4.41	9.00	4.41
	PGD(cm)	0.32	1.12	0.41
	Duration(s)	20.28	24.58	20.84
Marivan (MAR)	PGA(cm/s^2)	58.50	58.57	57.41
	PGV(cm/s)	4.52	6.67	4.79
	PGD(cm)	0.49	0.86	0.58
	Duration(s)	27.21	22.32	15.45

The use of strong ground motion simulation methods helps us understand the process of earthquakes, ground motion characteristics and predict future events. In this study, two synthesizing methods have been successfully applied in earthquake source simulation. The use of the EGF method in regions with unknown velocity structures is useful in solving the seismic problem because a small event as an Empirical Green Function represents the impulse response of the earth to seismic waves. However, one of the limitations of using this method is the lack of recording small events in seismic or ground motion stations. In this case, other simulation approaches such as the SFF method can be used alongside this technique. Using the SFF method requires detailed knowledge of the ray path, which is often not available. Consequently, different methods of simulating seismic events should be applied in such a way that they complement each other and compensate for the limitations of other approaches. We tested these techniques by comparing the synthetic and the observed records from the Ezgeleh earthquake (Mw=7.3). The comparison suggests that these methods are effective at simulating near-source ground motions in a broad-frequency range of engineering interest. The simulated strong ground motions in comparison with the observed ones show good agreement. However, some waveforms are underestimated or overestimated and the simulated ground motions can mostly explain major characteristics of the observed records. It can be seen there are differences between the synthesized diagrams and the observed ones. The contrasts between the graphs stimulated by EGF and observed ones are seen because the seismological structures around the epicenters are undefined and site effects in both events were assumed to be the same; besides, the site effects on stations have not been eliminated. However, the values of maximum acceleration resulting from simulations are rather close to the observed ones. Some of the mismatches between the diagrams could be because EGFs are recordings of actual earthquakes band limited by cultural noise and instrumental response. In addition, the EGF method assumes that the two events have the same hypocenter. Therefore, in this technique, the focus is on a

comparison between the peak values of observed records and the simulated diagrams. It is demonstrated in the results that mostly the PGA values have good agreement with the observations at different stations (figure 5). In this study we applied Haskell's (1964) rupture model, in which rupture velocity and rise time are assumed to be constant; also, the applied simulation methods use a simplified model of the rupture and propagation processes. The simplifications could cause some dissimilarity between the simulated and observed results. These dissimilarities are noticeable in the Fourier spectra, especially at the lower frequencies (figure 6) and in the duration of simulated records (table1). In addition, the simulated results can be improved by applying more detailed path effects and site amplification and considering the complexity of the rupture process.

4. Conclusion

On November 12, 2017, an earthquake in Kermanshah, Iran (in the Zagros seismotectonic zone) with a moment magnitude of 7.3 has been the largest event in this region in the last hundred years. The effect of the directivity in this event is visible. The rupture was initiated from Ezgeleh and propagated unilaterally along the southeast towards Sarpol-e Zahab city. The existence of long-period pulses in the record of the SPZ station and the maximum acceleration registered at this station, confirm the directivity of this earthquake. The estimated fault plane solution shows a reverse mechanism with a small strike-slip component for this event with the North West-South East trend, which is in agreement with the trend of faults in the region. In addition, the high scattering of the aftershocks could be an indicator of the low angle fault plane and the result of multiple small ruptures. We determined the strike, dip, and rake of the causative fault of the earthquake as 348, 27, and 137degrees, respectively. One of the complexities of the 2017 Ezgeleh earthquake and its aftershocks is that the causative fault of the earthquake was unmapped; also it seems several parallel faults have been activated in these events, so it calls for further studies in this region. Despite the complexities of this earthquake, the simulated results obtained by applying these two methods are compatible with the observed records of this event. The results show that the strong ground motions can be explained by the average fault rupture model. The Ezgeleh earthquake changed the expectations about the seismic behavior in this region. This earthquake, which is located within the Zagros fold and thrust belt with such magnitude, had not been anticipated before. With the information and data obtained from the events of this region in the last three years, more comprehensive studies can be done in this area. Also, this earthquake shows us that in areas with tectonics and seismic behavior similar to those of the Zagros fold and thrust belt, the possibility of destructive earthquakes is not unexpected. Therefore, it is necessary to simulate probable large earthquakes in this region and similar areas using different strong ground motion simulation techniques to design structures resistant to such earthquakes.

References

Alexander, N., Chanerley, A. & Goorvadoo, N., 2001. A review of procedures used for the correction of seismic data. 10.4203/ccp.73.39, 101-102.

Ambraseys, N.N. & Melville, C.P., 2005. A history of Persian earthquakes. Cambridge, UK, Cambridge University Press.

Berberian, M., 1995. Master "blind" thrust faults hidden under the Zagros folds active basement tectonics and surface morphotectonics. Journal of Tectonophysics, 241, 193-224.

Boore, D.M. & Bommer, J.J., 2005. Processing of strong-motion accelerograms: needs, options and consequences. Soil Dynamics and Earthquake Engineering, 25(2), 93-115. https://doi.org/10.1016/j.soildyn.2004.10.007

Campbell, K.W. & Bozorgnia, Y., 2006. Campbell-Bozorgnia NGA empirical ground motion model for the average horizontal component of PGA, PGV, PGD, and SA at selected spectral periods ranging from 0.01-10.0 seconds. Pacific Earthquake Engineering Research Center, Berkeley, CA.

Courboulex, F., Virieux, J., Deschamps, A., Gilbert, D. & Zoll, A., 1996. Source investigation of a small event using empirical Green functions and simulated annealing. Geophysical Journal International, 125, 768-780.

DeLorenzo, S., Filippucci, M. & Boschi, E., 2007. An EGF technique to infer the rupture velocity history of a smallmagnitude earthquake. J.Geophys. Res., 113, B10314, https://doi:10.1029/2007JB005496

Nissen, E., Tatar, M., Jackson, J.A. & Allen, M.B., 2011. New views on earthquake faulting in the Zagros fold-and-thrust belt of Iran. Geophysical Journal International, 186(3), 928-944, https://doi.org/10.1111/j.1365-246X.2011.05119.x

Hartzell, S., 1978. Earthquake aftershocks as Green's functions. Geophysical Research Letters, 5, 1-4.

Haskell, N.A., 1964. Total energy spectral density elastic of wave radiation from propagating faults. Bulletin of the Seismological Society of America, 54, 1811-1841.

Hutchings, L. & Viegas, G., 2012. Application of Empirical Green's Functions in Earthquake Source,

Wave Propagation and Strong Ground Motion Studies. In: D'Amico S. (Ed), Earthquake Research and Analysis – New Frontiers in Seismology. Lawrence Berkeley National Laboratory, USA, 87-140.

Hutchings, L., 1987. Modeling near-source earthquake ground motion with empirical Green's functions. Ph.D Thesis, State University of New York.

Imtiaz, A., Causse, M., Chaljub, E. & Cotton, F., 2015. Is Ground-Motion Variability Distance Dependent? Insight from Finite-Source Rupture Simulations. Bulletin of the Seismological Society of America, 105(2A), 950-962.

Irikura, K., 1991. The physical basis of the empirical Green function method and the prediction of strong ground motion for large earthquake. Proceedings International workshop of seismology and earthquake Engineering, 89-95.

Irikura, K., 1984. Prediction of strong ground motions using observed seismograms from small events. Proceedings of the 8th World Conference on Earthquake Engineering, 2, 465-472.

Jackson, J. & Fitch, T., 1981. Basement faulting and the focal depths of the larger earthquakes in the Zagros Mountains (Iran), Geophys. J. Int., 64, 561-586.

Karasözen, E., Nissen, E., Bergman, E.A. & Ghods, A., 2019. Seismotectonics of the Zagros (Iran) from orogen-wide, calibrated earthquake relocations. Journal of Geophysical Research: Solid Earth, 124, 9109-9129. https://doi.org/10.1029/2019JB01733

Honoré, L., Courboulex, F. & Souriau, A., 2011. Ground motion simulations of a major historical earthquake (1660) in the French Pyrenees using recent moderate size earthquakes. Geophysical Journal International, 187(2), 1001-1018. https://doi.org/10.1111/j.1365-246X.2011.05193.x

Mohammadi, F. & Moradi, A., 2019. The Double Difference Relocation of sequence of 2017 Ezgeleh earthquake. 8th International Conference on Seismology and Earthquake Engineering (SEE8), Nov 11-13, Tehran. Iran.

Motazedian, D. & Atkinson, G.M., 2005a. Stochastic finite-fault modeling based on a dynamic corner frequency. Bulletin of the Seismological Society of America, 95, 995-1010.

Motazedian, D. & Atkinson, G.M., 2005b. Earthquake magnitude measurements for Puerto Rico. Bulletin of the Seismological Society of America, 95, 725-730.

Motazedian, D. & Atkinson, G.M., 2005c. Ground-motion relations for Puerto Rico. Geological Society of America, 385, 61-80.

Niazi, M., Asudeh, I., Ballard, G., Jackson, J., King, G. & McKenzie, D., 1978. The depth of seismicity in the Kermanshah region of the Zagros Mountains (Iran). Earth and Planetary Science Letters, 40(2), 270-274.

Raghukanth, S.T.G., 2008. Modeling and synthesis of strong ground motion. Journal of Earth System Science, 117, 683-705.

Rezapor, M., Rezaee, R. & Tabatabaiy, S., 2018. Estimation of coda wave attenuation in the Kermanshah. 18th Iranian Geophysics Conference, Tehran, Iran, 509-512.

Road, H., 1973. Iranian Strong Motion Network (ISMN). Road, Housing & Urban Development Research Center, https://doi.org/10.7914/SN/I1

Shakal, A.F. & Bernreuter, D.L., 1980. Empirical analyses of near-source ground motion. United States.

Somerville, P., Irikura, K., Graves, R., 1999. Characterizing crustal earthquake slip models for the prediction of strong ground motion. Seismological Research Letters, 70(1), 59-80.

Talebian, M. & Jackson, J., 2004. A reappraisal of earthquake focal mechanisms and active shortening in the Zagros mountains of Iran. Geophys. J. Int., 156, 506-526.

Wan, K., Sun, X., Liu, Y., Ren, K., Sun, X. & Luo, Y., 2022. Spatial Coherency Model Considering Focal Mechanism Based on Simulated Ground Motions. Sustainability Journal, 14. https://doi.org/10.3390/su14041989

Wu, F., 1978. Prediction of strong ground motion using small earyhquakes. In Proceedings of 2nd International Conference on Microzonation Nati, Sci. Found., San Francisco. California, 701-704.

Yoshida, K., Uchida, N., Kubo, H., Takagi, R. & Xu, S., 2022. Prevalence of updip rupture propagation in interplate earthquakes along the Japan trench. Earth and Planetary Science Letters, 578, 117306. https://doi.org/10.1016/j.epsl.2021.117306.